Lockheed Missiles & Space Company, Inc.

Research and Development 3251 Hanover Street, Palo Alto, California 94304

In reply refer to: LMSC/D866823

27 February 1984

National Aeronautics & Space Administration Goddard Space Flight Center Wallops Island, Virginia 23337

Attention:

Mr. Larry J. Early, Code 1021.0

Sounding Rocket and Balloon Projects Branch

Subject:

Contract NASS-23563, Cosmic X-Ray Telescope Experiment

Enclosure: (1) Final Report (ten copies)

1. Pursuant to Article XV, subject contract, submitted herewith are copies of the Final Report.

> LOCKHEED MISSILES & SPACE COMPANY, INC. Advanced Systems Division

1. R. Matron

A. R. Motroni Contract Administator

ARM: bw

NASA cc:

Goddard Space Flight Center

Wallops Island, Virginia 23337 (w/1 cy encl) Attn: John Brinton, A. Wayne Mears, Code 244.1

NASA

Goddard Space Flight Center

Greenbelt, Maryland 20771 (w/1 cy encl)

Attn: Patent Counsel, Code 204

WASA

Goddard Space Flight Center Greenbelt, Maryland 20771 (w/1 cy encl)

Attn: Publications Branch, Code 253.1

(NASA-CR-177914) COSMIC X-RAY TELESCOPE EXPERIMENT final Report (Lockfeed Missiles and Space Co.) 29 p

N87-70381

68138

Unclas 00/93 43707

1451 GR-177914

FINAL REPORT

CONTRACT NAS5-23563

COSMIC X-RAY TELESCOPE EXPERIMENT

24 February 1984

R. C. Catura

Lockheed Palo Alto Research Laboratory

3251 Hanover Street

Palo Alto, California 94304

Table Of Contents

		Page			
ı.	Introduction	1			
II.	Aries 24.003	4			
	A. Experiment Payload	4			
	B. MSFC Calibration	5			
	C. Flight Results	8			
III.	Multilayer Studies				
IV.	Lacquer Coating				
v.	Nested Telescope Array				
VI.	Appendices				
	A. Cosmic X-ray Telescope for Aries Rocket Observations				
	B. Observations of the Iron				
	Emission Lines in the				
	X-ray Spectrum of the Supernova				
	Remnant Cassiopeia A.				
	C. Calculated Performance of a Wolter				
	Type I X-ray Telescope Coated by				
	Multilayers				

I. INTRODUCTION

The research funded under NAS5-23563 began in June of 1976 and was undertaken in cooperation with the Mullard Space Science Laboratory (MSSL) and the National Physical Laboratory (NPL), in the United Kingdom. The scientific objective of the investigation was to determine the spectra and angular structure of extended sources of cosmic X-ray emission. The technical objective of the research was to develop low cost methods for fabricating X-ray astronomical telescopes having angular resolution in the range of 15-20 arc sec. The approach has been to figure mirror blanks forged from aluminum alloy by the process of diamond-turning. This technique uses a high precision air-bearing lathe and a single crystal diamond as a machine tool. This figuring is done with an accuracy of $\frac{+}{-1}$ micron of the required curve and a surface finish of a few microinches rms.

A Wolter type I X-ray telescope having a single paraboloid-hyperboloid mirror pair was fabricated, calibrated at the Marshall Space Flight Center 1000-ft X-ray beam line and flown on an Aries rocket from White Sands Missile Range in 1980. Since that flight the telescope has been redesigned (still using the original mirror-pair) to accept a total of six nested mirror-pairs. Mirror blanks for two of these mirror-pairs have been fabricated. One paraboloid has been figured by precision machining in the U.K. Science and Engineering Research Council's (SERC) diamond turning facility and the mating hyperboloid is now being diamond turned. Techniques for obtaining high X-ray reflectivity by surface finishing these diamond-turned optics with metallized lacquer coating have been studied under this contract. Also, the practicality of depositing multilayer diffraction coatings on the reflecting surface of a Wolter I telescope was investigated and the increase in effective area calculated.

Results of the above research will be presented in this report. In cases where the data have been published, preprints or reprints of the papers are attached as Appendices. Unpublished results are discussed in the main text of this report.

II. ARIES 24.003

A. Experiment Payload

Development of the experiment payload for 24.003 during the period 1976-1979 is described in a paper 1 published in Proceedings of the S.P.I.E. A reprint of this paper is included in this report as Appendix A and includes details of the experiment, the payload for Aries 24.003, design of the Wolter type I paraboloid-hyperboloid mirror-pair and its fabrication process. The work of electroless nickel plating, polishing, and subsequent assessment of the mirror quality by optical and metrological means have been published 2-4 by the National Physical Laboratory (NPL). Results of their work will be summarized in this report.

After being figured by diamond-turning at the Oak Ridge Y-12 plant, measurements of the circularity and the slope errors of the mirror were made at NPL. The mirrors had been supported during diamond-turning by potting them into a rigid closely fitting fixture using a rubber-gel compound. The NPL measurements indicated that the pressure of pumping the gel into the fixture had evidently stressed the mirrors slightly. This stress had not relaxed as anticipated during the period before the gel cured. The mirrors were figured successfully but upon removal from the fixture measurable and systematic distortions were observed at NPL. A four-fold azimuthal distortion of the figure was detected with a maximum amplitude of 20 microns. These measurements predicted a FWHM angular resolution of 29 arc sec.

The mirrors were plated with 25 microns of electroless nickel and polished with a pitch lap and abrasive compound. The surface finishes of the mirrors were investigated with a Nomarski micrograph. The paraboloid was observed to have a surface finish smoother than the 10 Å rms sensitivity of the instrument while the hyperboloid was found to have an rms roughness ~30 Å rms.

The paraboloid and hyperboloid were aligned and bolted together with their axes. oriented vertically while in a collimated beam of visible light. The mirror-pair was subsequently attached to a mounting ring which supported them in the

Aries payload. A cross-sectional drawing of the mirror assembly is shown in Figure 1 and a photograph of the mirrors attached to the support ring is shown in Figure 2. The parameters of this mirror-pair are given in Table 1.

Table 1

Aries X-ray Telescope Parameters

Paraboloid Entrance Radius: 32.73 cm Hyperboloid Exit Radius: 26.09 cm

Paraboloid-Hyperboloid Joint Radius: 30.83 cm Grazing Angle at Joint: 1.92°

Paraboloid Length: 58.42 cm Hyperboloid Length: 46.46 cm

Focal Length: 228.6 cm Geometrical Area: 380 cm²

Reflecting Surface: Nickel

B. MSFC Calibration

Prior to the launch of 24.003 the telescope was calibrated at the Marshall Space Flight Center in the 1000 ft X-ray beam line. During this calibration the telescope was pointed at an X-ray source, 1 mm in diameter, located at a distance of 1000 ft. When the focal plane is offset approximately 2 cm to compensate for this finite distance the 1 mm spot appears, to a very good approximation as a distant on-axis point source. The performance of the Aries telescope was then measured for X-ray energies of .277, .572, .705, .933, 1.5, and 2.05 keV. The calibration utilized the flight Imaging Proportional Counter⁵ (IPC) provided by the Mullard Space Science Laboratory (MSSL). Analysis of the effective area which the telescope mirror assembly presents to a distance onaxis X-ray source has been completed and the results are shown in Figure 3. These lid disks indicate the effective area calculated from the X-ray optical constants of the nickel surface while the crosses show the measured values. The statistical uncertainty in the measurements is negligible compared to the size of the data points. The calculated and measured data points at .277 keV disagree appreciably. This is a systematic effect due to some X-ray events at this energy falling below the lower level pulse amplitude discriminator at the IPC output and therefore failing to be counted. The measured effective area at

.933 keV falls well above the calculated value because this is in the vicinity of the L-shell X-ray absorption edges in the nickel reflecting surfaces where the optical constants are very poorly known. At .572, .705, 1.5, and 2.05 keV the measured values average 63% of those calculated. Since there are two reflections in the telescope, these data indicate the polishing process has achieved ~80% of theoretical reflection efficiency. ~

The point Spread Functions (PSFs) of the telescope (mirrors plus IPC) which were measured at the six X-ray energies indicated above are shown in Figures 4-9. The PSF at a given energy is obtained by determining the centroid of the X-ray source image and summing the counts in IPC pixels which lie within successive annuli of increasing radius. The total counts within each annulus is then divided by the number of pixels contributing to the sum to obtain the normalized point spread function. The PSFs are shown on semi-log plots where the horizontal coordinate, which is given in IPC pixels, corresponds to off-axis angle in the telescope field. Since each pixel is 14.8 arc sec in size, the entire plot covers the central ~.40 radius of the field. All of these point spread functions show the typical response of an X-ray telescope in having a very intense central core surrounded by a low intensity tail (down by a factor of $\sim 10^4$). It is quite apparent from comparing Figures 4 through 9 that the central core of the telescope PSF becomes broader at low energies. This is due to several factors: The IPC spatial resolution is limited by noise in the resistive sheet read-out so it degrades roughly as E-1. Also, the IPC has a 3-mm axial depth for X-ray absorption which produces an energy dependent image blur. Finally, a systematic error was introduced by a 1.6 mm deflection of the detector window by the 900 Torr interior pressure when the IPC was placed in vacuum. The focal plane, intended to be 1 mm behind the window, was instead 2.6 mm into the detector gas. This also produced increased image blur preferentially at low X-ray energies because of their shorter interaction length in the gas. The measured imaging properties of the telescope are summarized in Table 2. The IPC gain was varied during the course of the measurements to optimize pulse height of the different X-ray energies within the electronic window. Consequently, the data of Table 2 do not vary monotonically with X-ray energy. The IPC resolution, shown in column 3, has been calculated from a semi-empirical expression which was normalized to the values measured for a 100-micron diameter pencil beam at 1.5 and .277 keV.

Table 2
Telescope Image Blur Measurements

X-ray Energy (keV)	Measured Telescope FWHM (Arc Sec)	Calculatæd IPC FWHM (Arc Sec)	Measured Telescope Half Power Radius (Arc Sec)
0.277	104	86	70
0.572	57	46	45
0.705	80	59	5 5
0.933	64	45	47
1.5	43	30	58
2.05	49	30	75

As indicated above, it is difficult to determine the mirror resolution from the data of Table 2 above because of uncertainties in the image blurring by the IPC. However, it is possible to calculate an upper limit to the image blur from the mirrors using the data at 1.5 keV, where effects of IPC blurring are minimal. Assuming the image blur from the IPC and the mirror add in quadrature, we have taken the square root of the difference in the squares of columns 2 and 3 at 1.5 keV, to obtain an upper limit of 31 arc sec FWHM for blurring from the mirrors. We believe the effect of X-ray scattering is unimportant in this calculation since it involves only the core of the telescope response and attribute this image blur to figure errors in the mirrors. Since the design goal for the mirror angular resolution was a blur circle radius of 20 arc sec, it is very encouraging that the results of our first attempt at figuring by diamond-turning fall well within this value.

The rise in half power radii at 1.5 and 2.05 keV shown in Table 2 is likely due to X-ray scattering in the mirrors. The measurements show an increase with X-ray energy, that is characteristic of scattering, at a level well above any effects of image blurring in the IPC. As mentioned previously, Nomarski micrographs of the mirrors indicated the hyperboloid to have a surface roughness of ~30Å rms. The paraboloid, which benefited from the experience of polishing the hyperboloid, was considerably better with a roughness below the 10Å rms sensitivity of the Nomarski interferometer. It is therefore likely that most of scattering originates in the hyperboloid.

C. Flight Results

The Aries X-ray telescope developed under this contract was flown from White Sands Missile Range on 20 September 1980. The primary instrument in the experiment payload on Aries 24.003 was the imaging X-ray telescope of Wolter Type I design which images an area of the sky ~1° in diameter. Two gas scintillation proportional counters (GSPCs) were also included in the payload for complementary observations of X-ray spectra. The overall scientific objective of the experiment was to study the nature and evolution of various sources of cosmic X-ray emission. The observational data involves measurements of the position, spectra, and time variability of X-ray sources and the structure of extended emission in the 0.15 - 2 keV range with an angular resolution of ~30 arc sec and proportional counter spectral resolution. During the flight of 24.003, observations were made on three X-ray sources, the Crab nebula, Cas A and Cyg X-1. The Crab was observed to investigate the existence of a soft X-ray halo which was implied from earlier occultation measurements. The IPC on the Einstein Observatory was unable to do this measurement because the Crab was too bright. Cas A was observed to provide a spectral-spatial map with a factor of 3 better angular resolution than the Einstein IPC. Cyg X-1 provided a point source calibration for the telescope and an opportunity for measuring its spectrum with GSPCs. Also, three bright stars, gamma And, zeta Tau and beta Cas were observed during periods when the star tracker in the attitude control system acquired these stars for update of the gyro system. The GSPCs measured the X-ray spectra of these sources from 3 - 30 keV with an energy resolution (E/E) of .08 at 6 keV.

As mentioned earlier, the telescope has been developed in collaboration with MSSL and NPL in the United Kingdom. The GSPCS are provided jointly by MSSL and ESTEC, a laboratory of the European Space Agency, at Noordwijk, The Netherlands.

Both the IPC at the telescope focus and the two GSPCs acquired useful data throughout the flight. The IPC, however, experienced low level electrical interference during flight which resulted in the loss of appreciable data. This interference did not register on the coarse high voltage monitor (sensitivity ~20V) but could be detected on the fine monitor. These interference events were

observed approximately 100 times during the flight, resulting in the loss of data for about a .5 sec interval following each event. We interpret the interference as resulting from charge build-up on the IPC window. the window was not uniformly conducting and the high counting rate experienced from the Crab produced positively charged regions of the window which disturbed the IPC operations. Rapid discharge of these regions capacitively coupled to the high voltage monitor to produce the observed interference. Many events were encoded with maximum X or Y coordinates such that they fall along the edges of the field of the X-ray images. In spite of these problems images of the Crab and Cyg X-l were obtained and are shown in Figures 10 and 11. The scale of these images is 0.66 arc min per mm. The image of the Crab is consistent with the 2 arc min angular extent of this source, but because of the IPC encoding problems it is not possible to give credence to the asymmetry apparent in the image above the Crab. The problems with electrical interference and image encoding improved during the Cyg X-1 observation. The image of Cyg X-1 in Figure 11 is consistent within experimental uncertainties with the MSFC X-ray calibration data for a point source.

The aspect data from 24.003 was reduced and the rocket attitude during the flight has been measured with an accuracy of 15 arc sec. There is a steady drift in pointing of the telescope of 5 arc sec per second during all of the observations. This information was given to the GSFC ACS group and the problem has been understood and corrected. Corrections for this drift were applied to the images of Figures 10 and 11 during their reconstruction.

The two GSPC detectors performed very well during flight and obtained the spectra of all three X-ray sources. In the spectrum of Cas A the presence of two emission features were confirmed. The first is a strong blend of lines between 6.5 and 7.5 keV with the principal line resulting from the 1s-2p transition in Fe XXVI. Evidence for a weaker blend at higher energy from the 1s-3p transition in this ion was also found. A reprint of a paper describing these results is included in Appendix B of this report.

III. Multilayer Studies

Calculations have been made on the response of a Wolter Type I X-ray telescope whose reflecting surface has been coated by multilayers. The multilayers were designed to image high energy X-ray in a selected narrow band pass. When overcoated with a thin nickel layer it was found that the low energy response of the telescope could be preserved. Details of these calculations and their results are given in the paper attached to this report as Appendix C.

A large multilayer deposition facility funded by Lockheed as a fixed asset has begun operation in the summer of 1983. This facility has two planar magnetron sputtering devices with active target areas 10 cm wide and 1 meter long. It is specifically designed to deposit multilayers on the interior of Wolter I telescope mirrors up to 1 meter diameter and 0.7 meters in axial length. The first attempt at producing multilayers on small test samples has recently been made. X-ray reflectivity measurements indicate this trial run to be unsuccessful since no Bragg diffraction peak was detected. Research on multilayer deposition with this system is continuing under the Lockheed Independent Research Program.

IV. Lacquer Coating

Research has been funded under this contract to develop a technique for applying the X-ray reflecting surface on a large Wolter I telescope mirror by coating its surface with acrylic lacquer. The lacquer is then overcoated with a thin metal layer applied by vacuum deposition. This technique has been pioneered by Dr. Peter Serlemitsos of Goddard Space Flight Center who has proven its effectiveness on small segments of aluminum sheet used to fabricate a broad-band X-ray telescope.

Two major problems are involved in coating the mirrors being fabricated under this contract. First, to determine the techniques required to apply optical quality coatings on large surface areas. Second, how to metallize these large surface areas without damaging the surface quality of the lacquer.

Efforts were directed at producing experimental test samples, small enough to be conveniently measured with the same techniques that may be applied to the large mirrors.

Since the mirrors are very large, using controlled withdrawal from a lacquer bath (Serlemitsos technique) is impractical. Consequently, the preferred method is to seal the ends of a cylindrical Wolter I mirror so that it may be used as a self-contained vessel. The mirror is then placed with its axis vertical, filled with lacquer and subsequently evacuated in a well-controlled manner. The lacquer should be thick enough to coat irregularities in the diamond-turned surface of the mirror but thin enough to allow surface tension within the lacquer and adhesion to the aluminum substrate to dominate over the force of gravity until the coating dries. A series of experiments concluded that a 5 micron thickness was optimum. Since the angular resolution goal for the telescope is a point spread function with ≤ 15 arc sec FWHM, uniform lacquer coating thickness is very important. Consequently, coating tests were made by placing samples in a reservoir, filling it with lacquer and pumping the lacquer out of this reservoir at a uniform rate. The test samples were made from 5 inch x 8 inch plate glass, that was 1/4 inch thick, which had been half silvered. Uniformity of the lacquer thickness was investigated using interference fringes generated by monochromatic lines from a mercury vapor lamp reflecting off the lacquer surface and the underlying glass surface. The difference in lacquer thickness between each pair of fringes is approximately ~2500Å. Using the techniques described above we have been able to routinely deposit a lacquer coating uniform to within 2500 Å in the central 4 inches by 6 inches of a 5 x 8 inch sample. If slope errors from lacquer coating are to make negligible contribution to the telescope point spread function the thickness variation must be less than ~ one fringe per inch. This requirement has been greatly exceeded in our tests except within ~1 cm from the edges.

Lacquer coated test samples are metallized by vacuum deposition of nickel in the planar magnetron sputtering system described previously. A centerless rotation device is designed to alternately expose the substrates to materials sputtered by the two magnetrons for multilayer deposition. It will also be used to rotate the telescope mirrors before a single magnetron for uniformly depositing nickel over their surfaces. Lacquer coated microscope slides were metallized with

nickel in this system and their X-ray reflectivity was measured as a function of grazing angle at an energy of 0.93 keV. Figure 12 shows the results from two such samples compared to the reflectivity indicated by the solid line that was calculated from scattering factors given by Henke et al.⁶ One sample (open circles) shows good agreement with the calculations out to a grazing angle of 2°. Data from the second sample, indicated by squares, lie well below the calculated reflectivity. We attribute this low reflectivity, also observed in several other samples, to microscopic surface damage of the lacquer from heating by electrons lost from the magnetron glow discharge. Deposition tests are continuing and we are confident of solving this problem.

V. Nested Telescope Array

The presently funded program under contract NASS-23563 involves fabricating two additional mirror-pairs. These mirrors are designed to be nested inside the Aries telescope flown on 24.003. Parameters of the complete mirror array for the Aries telescope are given in Table 3. This configuration is indicated

Table 3
Aries Mirror Parameters

	Nominal			
Mirror	Joint Radius (cm)	Grazing Angle (degrees)	Geometrical Area (cm²)	
1 ^a 2 ^b 3 ^c 4 ^d 5 ^d	43.3	2.64	730	
2 ^b	37.0	2.27	550	
3 ^C	31.3	1.92	290*	
4 ^d	26.1	1.61	260	
5ª	21.3	1.32	180	
6 ^a	16.9	1.04	110	

a Mirror-pairs presently funded under NAS5-27900.

in Figure 13, where the three mirror-pairs presently available or fabricated to the point of diamond-turning are shown cross-hatched. The remaining mirrors are

This space provided for potential flight of a mirror-pair being fabricated by Dr. Gordon Garmire.

Existing mirror-pair flown on 24.003.

Mirror-pairs fabricated under the present contract.

^{*} Includes effect of vignetting from paraboloid-hyperboloid separation.

for future expansion of the telescope. The mirror support plate, located between the mirror-pairs, has been designed to accept a mirror-pair presently being fabricated by Gordon Garmire at Penn State University (PSU). In reference to the central support plate, the upper part of Figure 13 is a section of six radial support ribs, while the lower half indicates a section of the X-ray transmitting portion of the plate. The central support plate also serves as an alignment fixture for the nested array. This alignment is obtained by utilizing the precision machining capability of the diamond-turning facility to machine the mating surfaces of the paraboloids, hyperboloids, and the support plate. The mating flange surfaces of each mirror are machined at the same time as its interior surface is figured and thus the flange and its outside diameter provide a true reference for the mirror axis. Surfaces of the support plate are diamond-turned to be flat and parallel, for axial positioning of the mirrors and angular alignment of their axes. The inner surfaces of raised lugs, shown in the top half of Figure 13, present on the six radial webs are also diamondturned to provide mirror alignment in a direction normal to the telescope axis. This alignment technique utilizes the precision of the diamond-turning machine to greatly reduce what otherwise would be a time consuming and expensive alignment effort in the telescope production process.

The outer cross-hatched mirror-pair is that from the telescope flown on Aries 24.003. As shown in Figure 1 these mirrors are designed to have the paraboloid and hyperboloid flanges joined. The 3.8 cm separation required for the support plate in Figure 13 has the effect of shifting the focal length of this mirror-pair from 228.6 cm to 231.4 cm. Also, approximately 20% of the hyperboloid area is vignetted for on-axis rays. The image blur, however, is increased by only a few arc sec. Accepting this slight degradation in performance allows the existing mirror to be used in the new configuration, where the focal length is 231.4 cm measured from the center of the support plate.

Lockheed's responsibility (machining up to the point of diamond-turning) for the portion of the telescope indicated by cross-hatching in Figure 13 has been completed under the present contract. The calculated effective area for the nickel surfaces of this 3-mirror telescope, not including IPC efficiency, is shown in Figure 14. Addition of the inner two mirror-pairs for 24.011 is expected to nearly double the area of the 24.003 mirror below the nickel L absorp-

tion edges at 0.85 keV and increase the effective mirror area at 1.5 keV by over a factor of 5.

We are confident of improving the figuring of future mirrors by changes in the fixturing for diamond-turning. The previously fabricated mirrors were potted in a massive support fixture, prior to diamond turning, using a rubber gel compound. However, during the potting process the mirror was stressed slightly. After diamond-turning, when the mirror was removed from the fixture, these stresses relaxed thereby distorting the figure. Mirrors which are fabricated in the future will be diamond-turned without such support fixtures as is now routinely done at the Lawrence Livermore Laboratory. Also, their figure will be measured in situ by a laser interferometer. The programmed curve followed by the diamond tool can then be modified to compensate for deviations due to deflection in the mirror blank and systematic errors in the slides of the diamond-turning machine. The paraboloid of mirror-pair 5 in Figure 13 has been successfully diamond-turned using these techniques.

Fabrication of mirrors 1 and 6 have been approved by NASA and will be completed under Contract NAS5-27900.

REFERENCES

- Catura, R. C., Acton, L. W., Berthelsdorf, R., Culhane, J. L., Sanford, P. W., and Franks, A., Proceedings of the SPIE, Vol 184, p 23, 1979.
- 2. Stedman, M., Proceedings of the SPIE, Vol 136, p 2, 1978.
- 3. Franks, A., Low Energy X-ray Diagnostics Proceedings, AIP Conference Proceedings, No. 75, edited by Atwood, D. T. and Henke, B. L., AIP, New York, p 179, 1981.
- 4. Stedman, M., Proceedings of the Conference on X- and Gamma-ray Imaging, Southampton, U. K., July 1983, to be published in Nucl. Instr. and Methods, 1984.
- 5. Stumpel, J. W., Sanford, P. W., and Goddard, H. F., Journal of Physics E, Scientific Instruments Vol 6, p 397, 1973.
- 6. Henke, B. L., Lee, P., Tanaka, T. J., Shimabukuro, R. L., and Fujikawa, B. K., Atomic Data and Nuclear Data Tables, Academic Press,, New York, 1982.

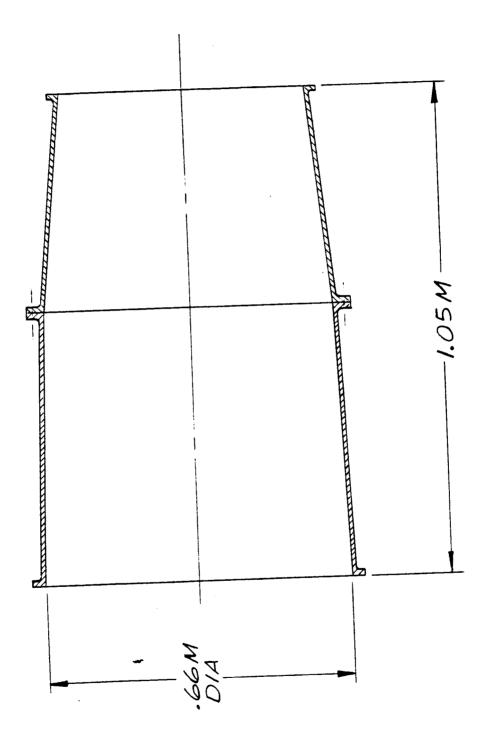


Figure 1. Cross-sectional drawing of the Aries 24.003 mirror assembly



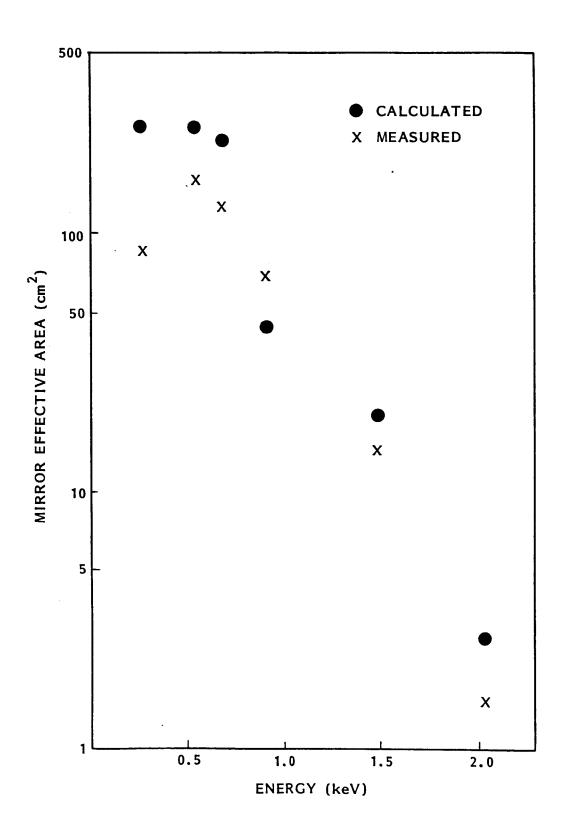


Figure 3. Effective area which the Aries mirror presents to a distant X-ray source on the telescope axis.

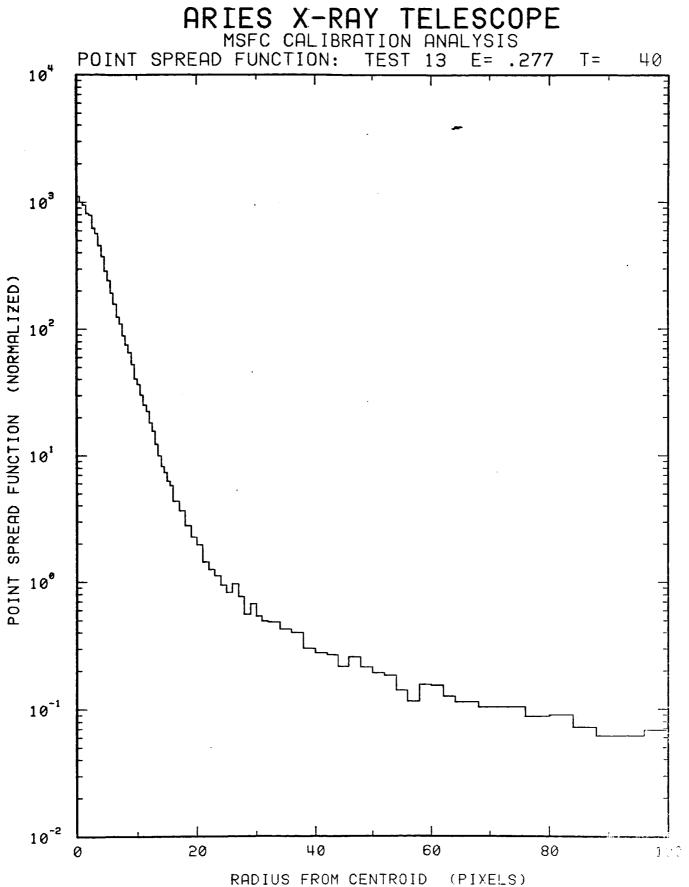


Figure 4. Telescope PSF at .277 KeV

PLU.

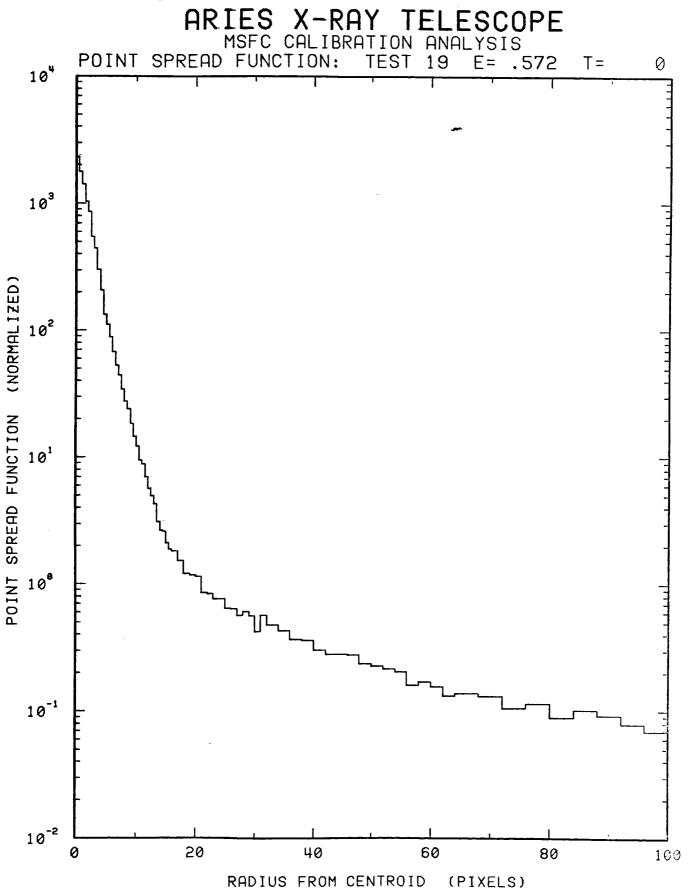


Figure 5. Telescope PSF at .572 KeV

ARIES X-RAY TELESCOPE MSFC CALIBRATION ANALYSIS POINT SPREAD FUNCTION: TEST 22 E= .705 **T** = 40 104 103 POINT SPREAD FUNCTION (NORMALIZED) 10² 101 100 10-1

Figure 6. Telescope PSF at .705 KeV

60

(PIXELS)

40

RADIUS FROM CENTROID

80

100

10-2

PLOT NO. 2 DONE AT 18:37 ON WED, 18 MAI

20

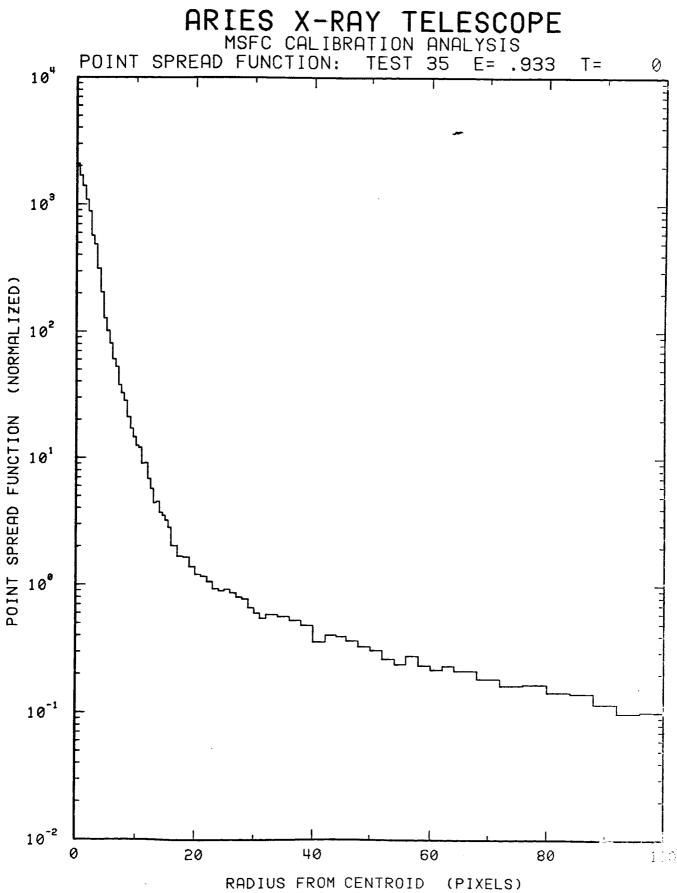


Figure 7. Telescope PSF at .933 KeV PLOT NO. 2 DONE AT 13:44 ON THU, 19 MAR.

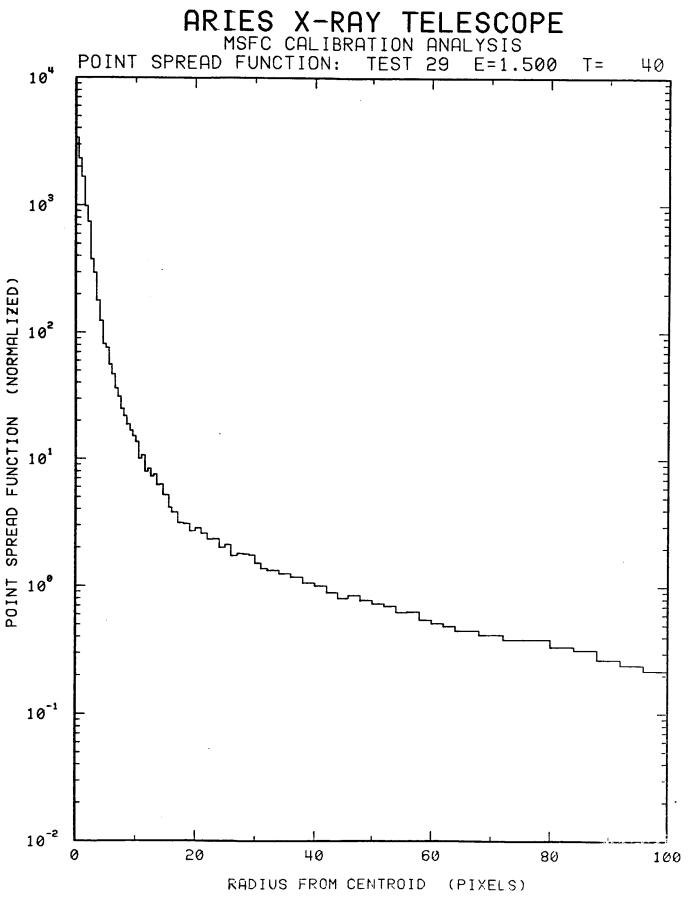
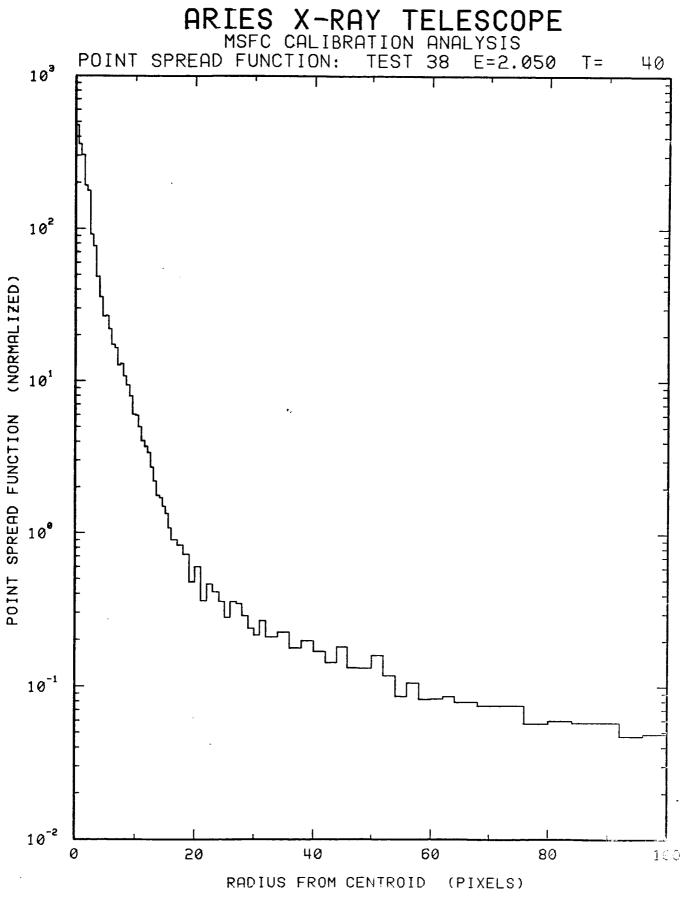


Figure 8. Telescope PSF at 1.5 KeV



PLOT NO. 2 DONE AT 16:01 ON TUE, 17 MAR Figure 9. Telescope PSF at 2.05 KeV

ARIES 24.003 FLIGHT DATA CRAB NEBULA

ARIES 24.003 FLIGHT DATA CYGNUS X-1

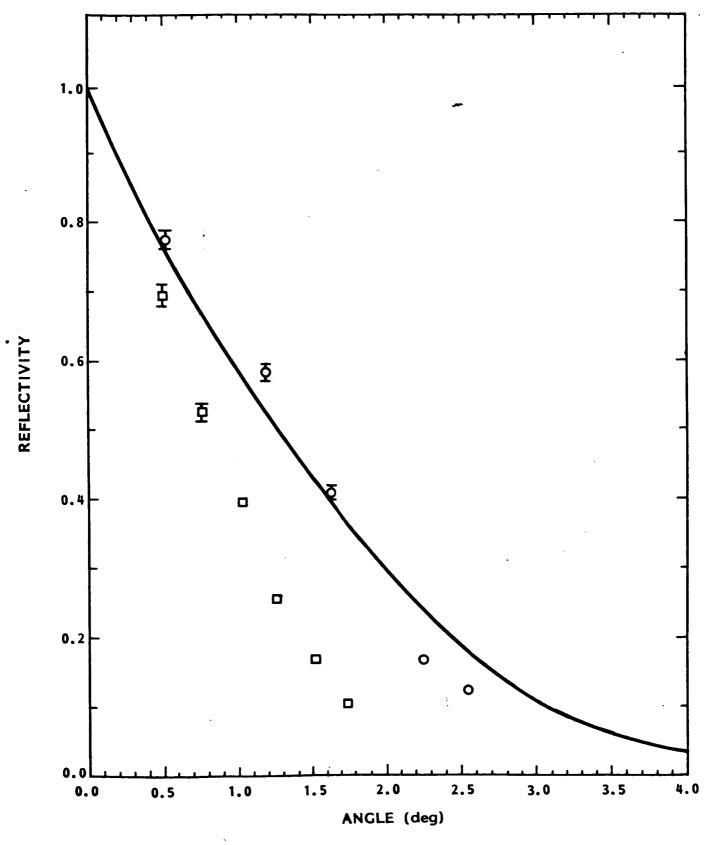


Figure 12. X-Ray Reflectivity of a Nickel-Coated Lacquer Sample

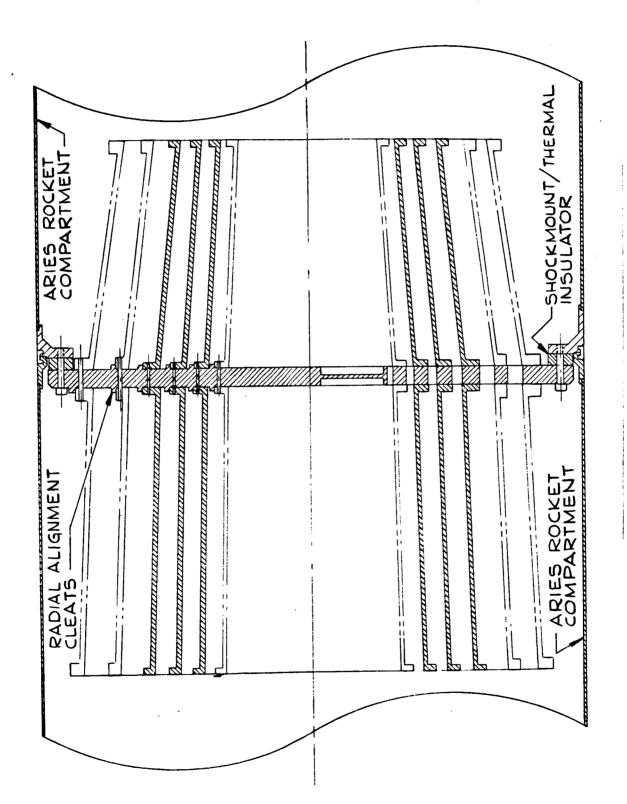


Figure 13. Cross-Section of the 6-mirror Aries Telescope

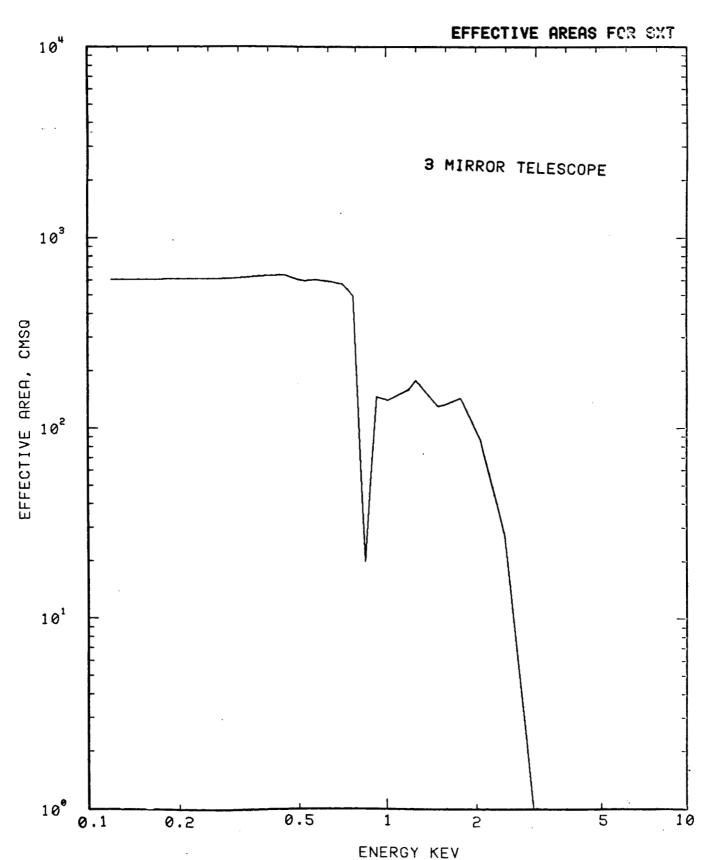


Figure 14. Calculated effective area of the cross-hatched 3-mirror